CSIRO PUBLISHING www.publish.csiro.au/journals/eg Copublished paper, please cite all three:
Exploration Geophysics, 2009, **40**, 114–120; *Butsuri-Tansa*, 2009, **62**, 114–120; *Mulli-Tamsa*, 2009, **12**, 114–120

A new waveform inversion method to determine the rupture directivity of moderate earthquakes: numerical tests for rupture models

Seung-Hoon Yoo[1] Junkee Rhie[1,2]

[1]School of Earth and Environmental Science, Seoul National University, Seoul, South Korea.
[2]Corresponding author. Email: rhie@snu.ac.kr

Abstract. Rupture directivity is the important parameter in estimating damage due to earthquakes. However, the traditional moment tensor inversion technique cannot resolve the real fault plane or the rupture directivity. To overcome these limitations, we have developed a new inversion algorithm to determine the moment tensor solution and the rupture directivity for moderate earthquakes, using the waveform inversion technique in the frequency domain. Numerical experiments for unilateral and bilateral rupture models with various rupture velocities confirm that the method can resolve the ambiguity of the fault planes and the rupture directivity successfully. To verify the feasibility of the technique, we tested the sensitivity to velocity models, which must be the most critical factor in practice. The results of the sensitivity tests show that the method can be applied even though the velocity model is not perfect. If this method is applied in regions where the velocity model is well verified, we can estimate the rupture directivity of a moderate earthquake. This method makes a significant contribution to understanding the characteristics of earthquakes in those regions.

Introduction

The size of an earthquake is theoretically proportional to the area of the fault where the effective slip occurs. Generally, the length of the fault is a few to several tens of kilometres for moderate earthquakes (Mw >5.0) and several tens to hundreds of kilometres for large earthquakes (Mw >7.0). As the effective faulting area increases, the effect of rupture directivity usually becomes significant. In cases of large earthquakes, rupture directivity is clearly one of the most important factors controlling damage due to earthquakes. While the effect of rupture directivity for moderate earthquakes is not as large as that for large earthquakes, it is still an important factor in characterising the pattern of radiated seismic energy. In other words, even moderate earthquakes can cause damage to specific areas due to the effects of rupture directivity (Shakal et al., 2006). Therefore, determination of the rupture directivity for moderate earthquakes is very important for estimating damage and providing basic information about the seismic hazard analysis in regions where large earthquakes are infrequent.

To determine the rupture directivity of moderate earthquakes, we have developed a new waveform inversion method. Waveform inversion techniques have been widely used for estimating the source parameters of earthquakes and can be roughly classified into two approaches, based on the assumption of the source dimension: one is the point-source approach, and the other is the finite-fault approach. The former approach can rapidly provide the scalar moments, focal mechanisms, and centroid depths of the earthquakes (Dziewonski et al., 1981; Dziewonski and Woodhouse, 1983; Dreger and Helmberger, 1993; Zhao and Helmberger, 1994). However, this approach inherently cannot resolve the actual fault plane or rupture directivity. The latter approach was first suggested by Hartzell and Helmberger (1982) and Hartzell and Heaton (1983) to overcome the limitation of the former approach by introducing the concept of the finite fault. This approach has the advantage of providing information about the detailed rupture characteristics of the events, including the rupture directivity. However, this approach requires precise Green's functions to obtain reliable solutions. Our new inversion method is based on the point-source approach, but the method is designed to invert waveforms for the moment tensor solution and the source time function at each station simultaneously. Since the source time function contains information about the rupture characteristics of the event, it is possible to resolve the actual fault plane and estimate the rupture directivity by analysing them at stations with good azimuthal coverage (Haskell, 1964; Lay and Wallace, 1995).

Before applying the method to real earthquake data, we performed numerical experiments to verify our new method. We also performed tests for sensitivity to the velocity structure, which can cause errors in real applications. Our numerical results show that the method can be applicable when the velocity structure is well defined.

Modified centroid moment tensor inversion in the frequency domain

The kth component of the displacement waveforms, u_k, for a point dislocation source can be represented in the frequency domain by

$$u_k(\mathbf{x}_s, \omega) = S(\mathbf{x}_s, \omega) \sum_{j}^{3} \sum_{i}^{3} G_{ki,j}(\mathbf{x}_s, \omega) \cdot M_{ij}, \qquad (1)$$

where the suffixes i and j denote the direction components in Cartesian coordinates. $G_{ki,j}$ is a derivative with respect to the source coordinate j of G_{ki}, which is the kth component of the Green's function due to the ith directional force (Aki and Richards, 2002). S and M_{ij} are the source time function and the moment tensor, respectively. We assume that the source depends on the position of station $\mathbf{x}_s$ to consider the effects of the rupture directivity.

To obtain the optimal source time function from three-component waveforms, we modified the representation of the

 10.1071/EG08109 0812-3985/09/010114

source time function introduced by Shin et al. (2007). Here, we assumed that the source time functions for all three components at each station are consistent with each other. In our parameterisation, the complex source time functions are separated by two parts, real and imaginary, for each station and frequency component (Shin et al., 2007):

$$S(\mathbf{x}_s, \omega) = \mathrm{Re}\{S(\mathbf{x}_s, \omega)\} + i\mathrm{Im}\{S(\mathbf{x}_s, \omega)\}. \quad (2)$$

Basically, we assume a pure double-couple source for the earthquake and a time-invariant focal mechanism during the propagation. Therefore, the moment tensor matrix can be represented by five independent elements, such as M_{xx}, M_{yy}, M_{xy}, M_{xz}, and M_{yz}. The total number of source parameters is $5 + 2 \times$ (number of stations) $\times$ (number of frequencies) in the inverse problem.

The moment tensor is the lower-frequency characteristic of the source. However, the rupture directivity or the source time function is the higher-frequency characteristic. Because high-frequency waveforms are very complex and strongly affected by the Earth's structure, a higher-frequency source characteristic requires a more accurate velocity structure than a lower-frequency source characteristic (Dreger and Helmberger, 1993). Thus, we separate the inversion sequences and source parameters to enhance the stability of the solution by using different frequency bands. We invert the lower-frequency waveforms for the moment tensor solution, whereas we invert the higher-frequency waveforms for the source time function based on the moment tensor solution obtained from lower-frequency waveforms. Objective functions are constructed from a L_2-norm between the pre-filtered synthetic data u_k and the observed data d_k in the frequency domain, giving

$$E_{\mathrm{mnt}} = \sum_{i\mathrm{stn}}^{n\mathrm{stn}} \sum_{k=1}^{3} \sum_{\omega}^{n\mathrm{freq}} \left(u_k^{i\mathrm{stn}}(\omega) - d_k^{i\mathrm{stn}}(\omega) \right)^* \left(u_k^{i\mathrm{stn}}(\omega) - d_k^{i\mathrm{stn}}(\omega) \right), \quad (3)$$

and

$$E_{\mathrm{src}}(\omega) = \sum_{i\mathrm{stn}}^{n\mathrm{stn}} \sum_{k=1}^{3} \left(u_k^{i\mathrm{stn}}(\omega) - d_k^{i\mathrm{stn}}(\omega) \right)^* \left(u_k^{i\mathrm{stn}}(\omega) - d_k^{i\mathrm{stn}}(\omega) \right), \quad (4)$$

where E_{mnt} and E_{src} are the objective functions for the moment tensor inversion and the source time function inversion. The superscript * denotes the complex conjugate operator. We used 0.05–0.1 Hz and 0.05–1.0 Hz pass bands for the moment tensor inversion and the source time function inversion, respectively.

To solve the inverse problem, we use the full Newton method. Newton's method is derived from a Taylor series expansion (up to quadratic order) of the objective function to be minimised (Bertsekas, 1982; Tarantola, 1987).

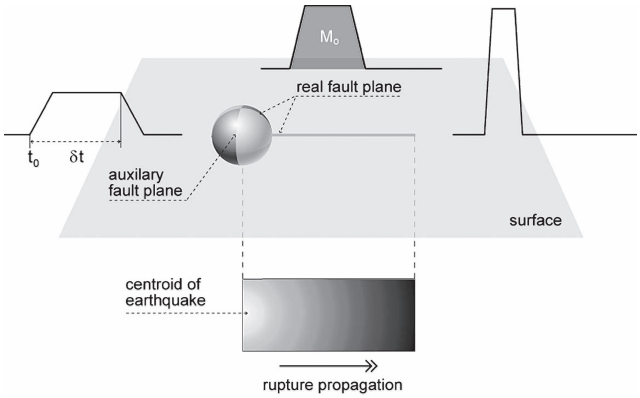

Fig. 1. Illustration of the azimuthal variability of the source time function for unilateral rupture faulting. In the moment tensor solution, the beach ball has two theoretical fault planes, the real and the auxiliary fault plane.

Source time function and rupture directivity

The duration, δt, of the source time function in the Haskell model (Haskell, 1964) can be expressed as a function of the angle θ between the station and the rupture direction, the length of the fault, L, the rupture velocity, v_r, and the phase velocity in the medium, c (Lay and Wallace, 1995):

$$\delta t = L\left(\frac{1}{v_r} - \Gamma\right), \quad \text{where } \Gamma = \frac{\cos\theta}{c}. \quad (5)$$

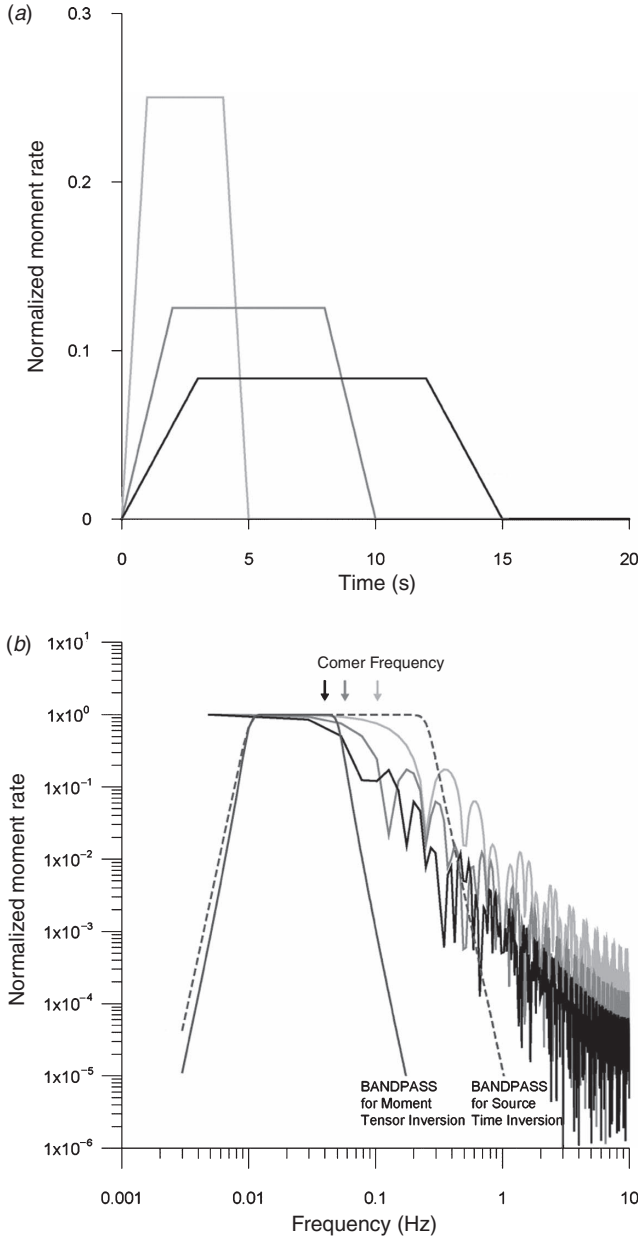

Fig. 2. Relationship between the duration and the corner frequency of the source time function: (*a*) Source time functions with different durations, and (*b*) amplitude spectrum of the source time functions.

For a unilateral rupture, the source time function has a sharp and large peak in the direction of the rupture propagation but has a broad and small peak in the opposite direction (Figure 1). However, the area under the source time function is proportional to the seismic moment, which must be independent of the azimuth. Therefore, the source time functions have the same area for the same event regardless of the azimuths of the seismic stations. In other words, the amplitude spectrum has a higher corner frequency for the shorter source time duration but a lower corner frequency for a longer duration in the frequency domain (Figure 2). These characteristics can change the pattern of the radiated energy for the earthquake. The radiated energy of the earthquake can be calculated by integration of the moment rate function in the frequency domain (e.g. Patton and Walter, 1993):

$$E_R \propto \int_0^\infty |\omega \dot{M}(\omega)|^2 d\omega. \quad (6)$$

We calculate the radiated energy using the source time function at each station and determine the direction of the fault and the rupture propagation direction from the analysis of the pattern of radiated energy.

Numerical tests

Before applying the method to real earthquake data, we verify the new algorithm using synthetic waveforms for imaginary earthquakes. The imaginary earthquake ($M_o = 1.0 \times 10^{25}$ dyne-cm, $M_w = 5.96$) used in numerical tests has a strike-slip mechanism (strike/dip/slip, 305°/90°/0°) and a hypocentral depth of 6 km (Figure 3). To simulate the rupture propagation effects, we assumed that the imaginary earthquake consists of 30 point sources distributed along the strike direction at intervals of 500 m. The epicentre is defined as the point where the rupture initiated (see Figure 3). All the point sources have the same size

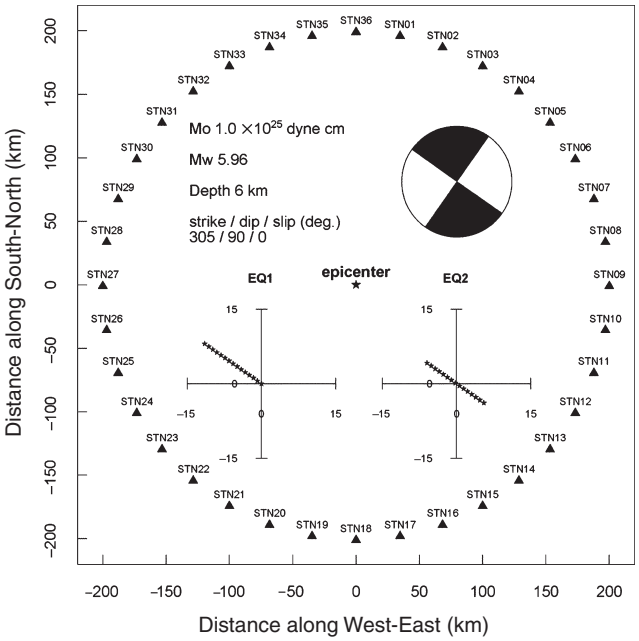

Fig. 3. Configuration of the numerical tests. EQ 1 has a unilateral rupture to the 305° direction, and EQ 2 has a bilateral rupture to the 125° and 305° directions. The beach ball represents the focal mechanism of the event. For all cases, the events have the same scalar moment, focal mechanism, fault length, and centroid depth.

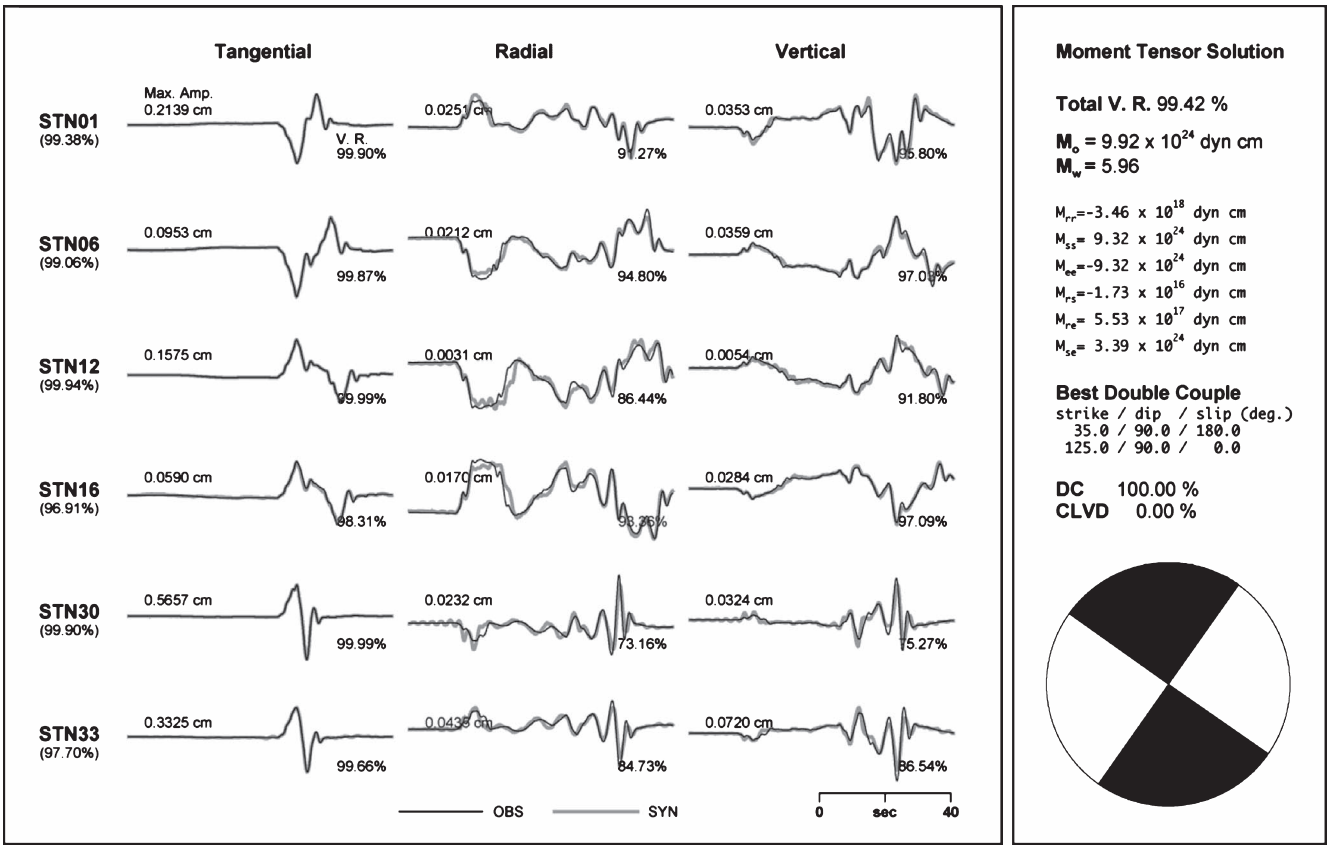

Fig. 4. The moment tensor solution for a unilateral rupture model with $v_r = 2.75$ km/s. The variance reductions calculated for each component and station. OBS indicates the synthetic waveform, and SYN denotes the best fitting waveform obtained from the inversion.

and mechanism. The synthetic waveforms at each station can be constructed by the summation of all synthetics for 30 point sources, after correcting for time delays due to rupture propagation. A constant rupture velocity was assumed, and a triangle source time function with 1-s duration was convolved to get the final synthetic data. We considered 36 artificial seismic stations located 200 km away from the epicentre. We tested two rupture models to evaluate our algorithm. Model EQ 1 is a unilateral rupture model, and the rupture direction is 305° from the epicentre. Model EQ 2 is a bilateral rupture model, and the rupture propagates in two opposite directions (125° and 305°) from the epicentre. In our numerical simulations, we tested various rupture velocities, such as 2.5 km/s, 2.75 km/s, 3.0 km/s, and 3.5 km/s, for the two models. For synthetic computation, we used the frequency-wavenumber integration method and the 1D velocity model used to test the synthetic method (Saikia, 1994).

The results of the numerical tests for the various rupture models confirm that the suggested method can easily determine the real fault plane and the direction of the rupture propagation. Since all experiments provide similar results, we give full details of one specific experiment. In case of EQ 1 with $v_r = 2.75$ km/s, the detailed procedures are as follows. First, we examined the result of the moment tensor inversion (see Figure 4). The total variance reduction between the synthetic and observed waveforms is 99.42%. For most stations, the values are very high (over 99%). Although we considered the Green's function only from the epicentre to the station in the inversion, instead of from the locations of the 30 point sources, the moment tensor solution we obtained is almost exactly the same as the one we assumed for the synthetics. In addition, the durations of the estimated source time functions are consistent with the theoretical ones calculated from the Haskell source model (see Figure 5*a*).

Then, we determined the real fault plane from two focal planes by analysing the pattern of the radiated energy calculated from EQ 6. The moment tensor inversion provides two focal plane solutions (strike/dip/slip, 35°/90°/180°, 125°/90°/0°). However, the calculated energy pattern has a significant maximum near 305° (the direction of the predetermined rupture propagation). From the trend of the energy pattern, we can easily resolve the real focal plane and rupture propagation direction of the EQ 1 model (125°/90°/0°). In the EQ 2 case, we also found that we can determine the actual fault plane and the direction of the rupture propagation (see Figure 5*c*).

Tests of sensitivity to velocity structures

Although the results of our numerical experiments in the previous section show that the method has the potential to be applicable to real earthquake data, we expect that there will be some obstacles in practice. Since the new algorithm requires high-frequency waveforms and they are relatively more sensitive to the velocity structure compared to low-frequency waveforms, we performed tests on sensitivity to the velocity structure, and evaluated how the inversion results can be affected by errors in the velocity structure. To conduct the sensitivity tests, we constructed several sets of velocity models by randomly perturbing the values of the velocity at each depth (see Figure 6). To find the maximum perturbation

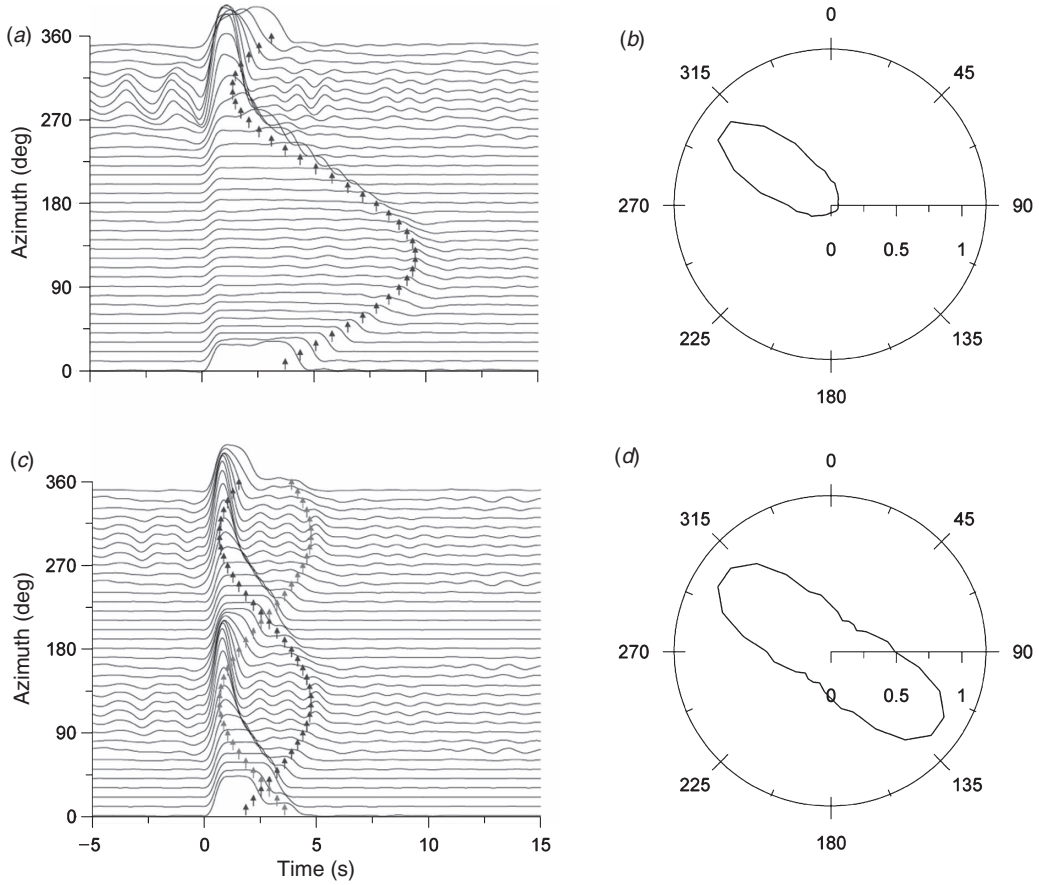

Fig. 5. Inverted source time functions (*a* and *c*) and radiation patterns of normalised energy (*b* and *d*) for EQ 1 (*a* and *b*) and EQ 2 (*c* and *d*) with $v_r = 2.75$ km/s. The black and grey vertical arrows represent the theoretical duration of the source-time functions.

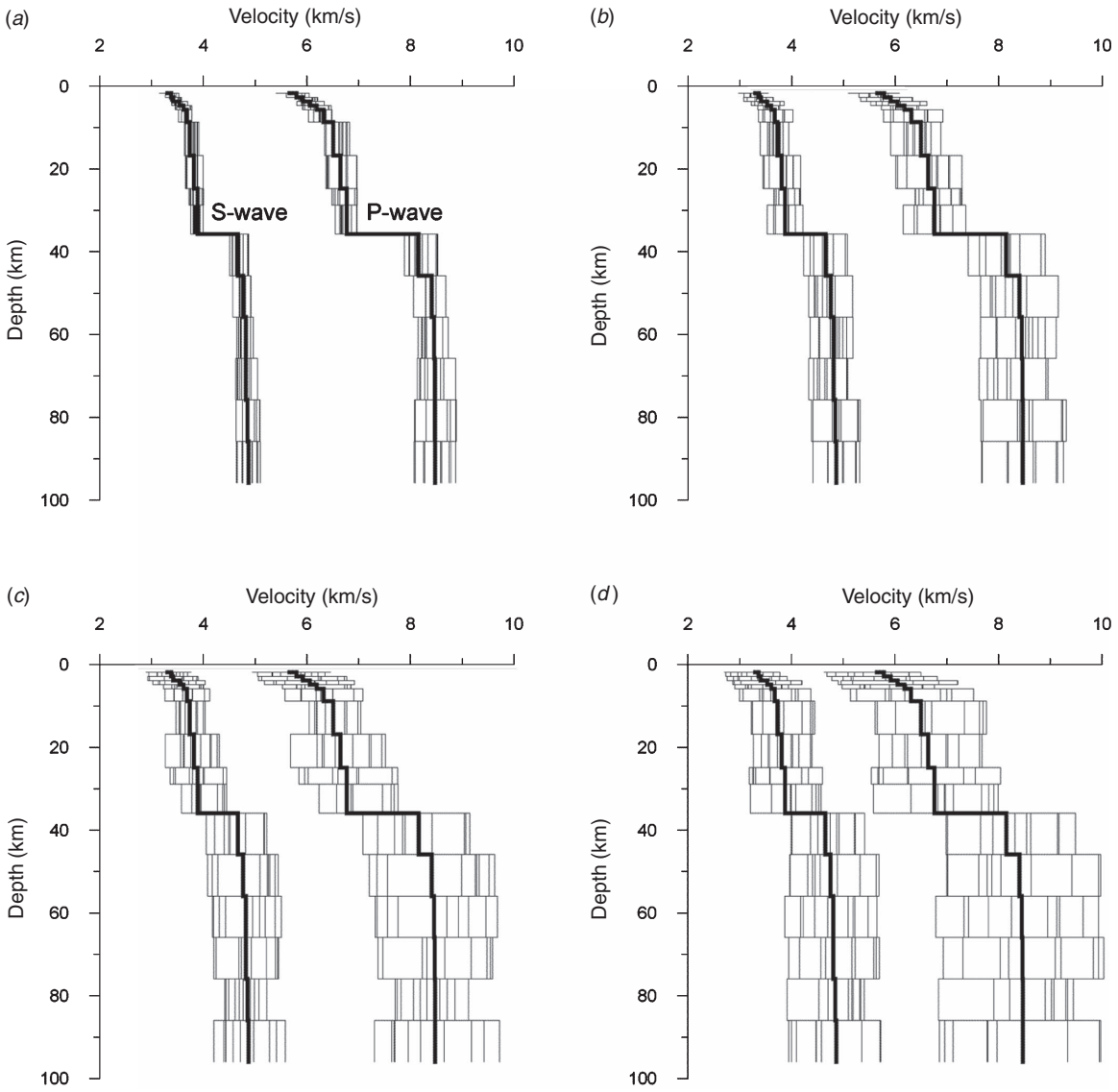

Fig. 6. Velocity models used in inversion. The bold lines are the true velocity model used in forward modelling to generate EQ 1 and EQ 2. The grey lines are the perturbed velocity models. The degree of velocity perturbation is (*a*) 5%, (*b*) 10%, (*c*) 15%, and (*d*) 20%.

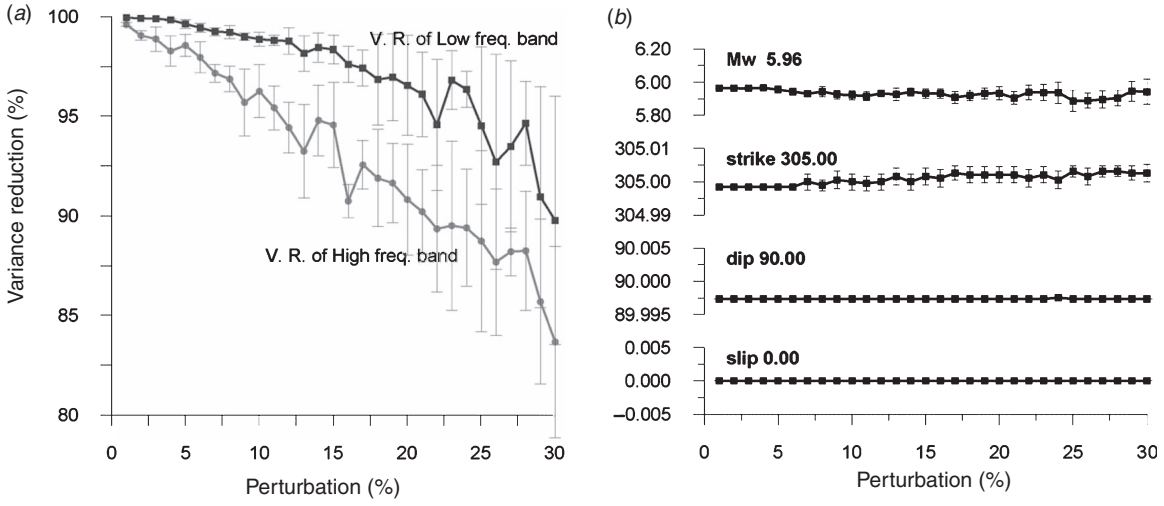

Fig. 7. Results of the sensitivity tests for the bilateral rupture model (EQ 2 with $v_r = 2.75$ km/s). (*a*) Variance reductions with respect to velocity perturbations. (*b*) Moment magnitudes and angles of the best double couple with respect to velocity perturbations. Error bars indicate 1 standard deviation.

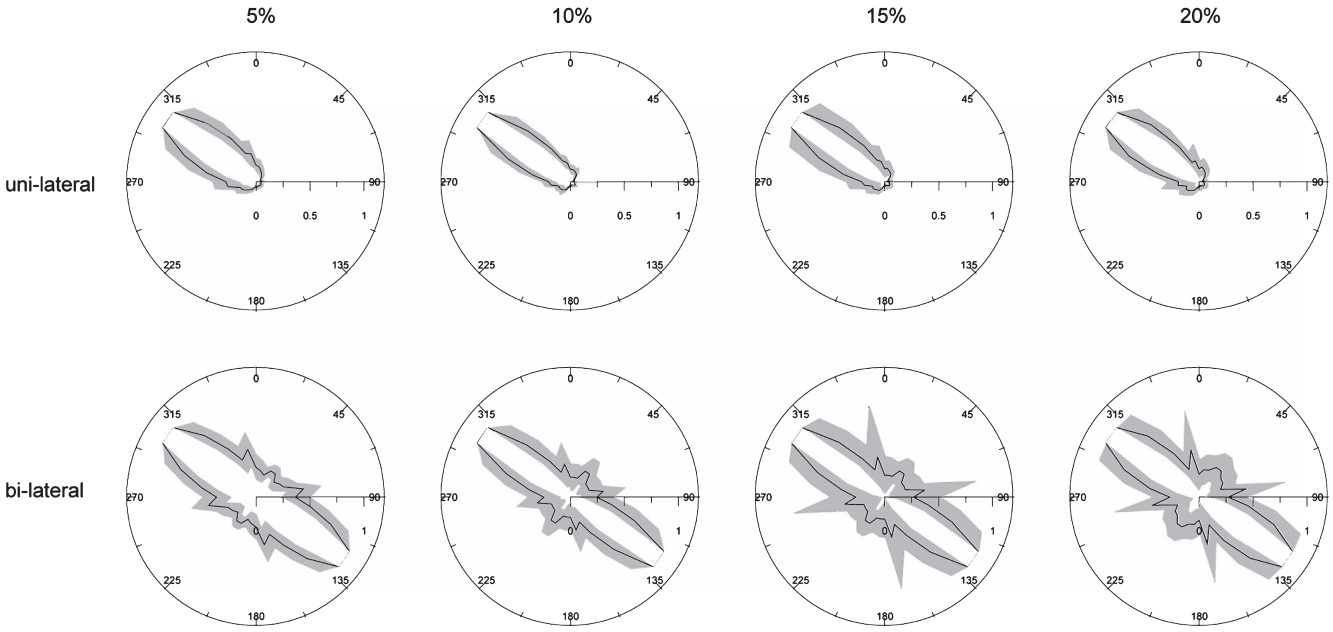

Fig. 8. Radiation patterns of normalised energy with respect to the rupture models and velocity perturbations. The black bold line represents the mean values, and the grey area represents 2 standard deviations with confidence of 95.45%.

that can provide a stable inversion result, several levels of perturbation were tested. We determined the source parameters for each velocity model using our inversion technique. The mean and standard deviations of the variance reduction, moment tensor solution, and radiated energy pattern were calculated for each level of perturbation.

As the level of perturbation increases, the variance reduction decreases but its standard deviation increases (see Figure 7*a*). The variance reductions in the low-frequency band are higher than the ones in the high-frequency band by ~1% to 5% and decrease more slowly. The moment tensor solutions are almost identical for all levels of the perturbations (see Figure 7*b*). As we expected, these results indicate that the long-period waveforms are less sensitive to the velocity structure.

Figure 8 shows the patterns of the radiated energy for the two rupture models. We can clearly see that the patterns deviate from the theoretical patterns as the level of the velocity perturbations increase because of the inaccurate Green's functions. For the unilateral rupture model, the rupture propagation direction can be well determined even though the level of the perturbation is up to 20%. However, the determination of the rupture propagation direction for the bilateral model is quite difficult if the velocity model is not accurate. The unrealistic peaks in the energy radiation pattern become significant when the level of the perturbation is larger than 10%. In a real earthquake, the rupture processes would be more complex than our models, and the station coverage would be far from perfect. Considering these difficulties, we can expect that an accurate velocity model is required for stable inversion results for real earthquakes.

Conclusions

In this study, we have suggested a new inversion algorithm to determine the rupture directivity of moderate earthquakes. Numerical tests with the two rupture models showed that the method can determine the moment tensor solution and the rupture propagation direction at the same time. The final goal of this study is to apply this method to real earthquake data and reveal the propagation direction. However, in practice, we can expect that there are many obstacles. It is certain that the most significant obstacle is the accuracy of the Green's function. In most waveform inversions, the accuracy of the Green's function is the main factor that controls the inversion result, and this is true for the method suggested in this study. The sensitivity tests for the velocity structure indicate that this method can determine the actual fault plane and the rupture propagation direction for both unilateral and bilateral rupture models if the error in the velocity model is small. As the velocity model deviates from the actual velocity structure, the rupture propagation direction becomes more difficult to determine. This effect is especially significant for the bilateral rupture case. This implies that there is a possibility that this method will not work for real earthquakes. However, the tolerable error in the velocity structure is ~10% to 15%. Getting this level of accuracy in the velocity model might be difficult, but it is definitely an achievable goal. If this method is applied to regions where the velocity models are well verified, we can estimate the rupture directivity of moderate earthquakes. This method can make a significant contribution to understanding the characteristics of earthquakes in those regions. In addition, this method may be able to provide preliminary information for large events before time-consuming finite-fault inversion results are available.

Acknowledgment

We thank Dong-Joo Min and Won Sang Lee for their helpful comments. S.-H. Yoo thanks Changsoo Shin for his advice and guidance in improving this paper. This work was funded by the Korea Meteorological Administration and Development Program under Grant CATER 2008–5113.

References

Aki, K., and Richards, P. G., 2002, *Quantitative Seismology*, 2nd Edition, University Science Books, Sausalito, 700 pp.

Bertsekas, D. P., 1982, Enlarging the region of convergence of Newton's method for constrained optimization: *Journal of Optimization Theory and Applications*, **36**, 221–251. doi: 10.1007/BF00933831

Dreger, D. S., and Helmberger, D. V., 1993, Determination of source parameters at regional distance with three-component sparse network data: *Journal of Geophysical Research*, **98**, 8107–8125. doi: 10.1029/93JB00023

Dziewonski, A. M., and Woodhouse, J. H., 1983, An experiment in systematic study of global seismicity: centroid moment solutions for 201 moderate and large earthquakes: *Journal of Geophysical Research*, **88**, 3247–3271. doi: 10.1029/JB088iB04p03247

Dziewonski, A. M., Chou, T. A., and Woodhouse, J. H., 1981, Determination of earthquake source parameters from waveform data for studies of global and regional seismicity: *Journal of Geophysical Research*, **86**, 2825–2852. doi: 10.1029/JB086iB04p02825

Hartzell, S. H., and Helmberger, D. V., 1982, Strong-motion modeling of the Imperial Valley earthquake of 1979: *Bulletin of the Seismological Society of America*, **72**, 571–596.

Hartzell, S. H., and Heaton, T. H., 1983, Inversion of strong ground motion and teleseismic waveform data for the fault rupture history of the 1979 Imperial Valley, California, earthquake: *Bulletin of the Seismological Society of America*, **73**, 1553–1583.

Haskell, N. A., 1964, Total energy and energy spectral density of elastic wave radiation from propagating faults: *Bulletin of the Seismological Society of America*, **54**, 1811–1841.

Lay, T., and Wallace, T. C., 1995, *Modern Global Seismology*, Academic Press.

Patton, H. J., and Walter, W. R., 1993, Regional moment: magnitude relations for earthquakes and explosions: *Geophysical Research Letters*, **20**, 277–280. doi: 10.1029/93GL00298

Saikia, C. K., 1994, Modified frequency-wavenumber algorithm for regional seismograms using Filon's quadrature; modeling of Lg waves in Eastern North America: *Geophysical Journal International*, **118**, 142–158. doi: 10.1111/j.1365-246X.1994.tb04680.x

Shakal, A., Haddadi, H., Graizer, V., Lin, K., and Huang, M., 2006, Some Key Features of the Strong-Motion Data from the M 6.0 Parkfield, California, Earthquake of 28 September 2004: *Bulletin of the Seismological Society of America*, **96**, s90–s118. doi: 10.1785/0120050817

Shin, C. S., Pyun, S., and Bednar, J. B., 2007, Comparison of waveform inversion, part1: conventional wave field vs logarithmic wave field: *Geophysical Prospecting*, **55**, 449–464. doi: 10.1111/j.1365-2478.2007.00617.x

Tarantola, A., 1987, Inverse Problem Theory: Methods for Data Fitting and Parameter Estimation, Elsevier.

Zhao, L. S., and Helmberger, D. V., 1994, Source estimation from broadband regional seismograms: *Bulletin of the Seismological Society of America*, **84**, 91–104.

Manuscript received 17 November 2008; revised manuscript received 23 December 2008.

중간 규모 지진의 단층 파쇄 방향성 결정을 위한 새로운 주파수 영역 역산방법: 파쇄 전파 모델을 이용한 수치 시험

유승훈[1], 이준기[1]

1 서울대학교 지구환경과학부

요 약: 단층 파쇄의 방향성은 지진 피해를 평가하는데 있어 매우 중요한 지진원 특성이다. 하지만 기존의 모멘트 텐서 역산 방법으로는 단층의 파쇄 방향은 물론 실제 단층면의 방향도 정확하게 결정하기 어렵다. 본 연구에서는 중간 규모의 지진에 대하여 주파수 영역 파형 역산 방법을 이용하여 모멘트 텐서와 단층 파쇄의 방향성을 동시에 역산하는 방법을 제안하였다. 여러 가지 다양한 파쇄 전파 모델을 가정한 수치 실험을 통해 역산 방법을 검증하였고, 실제 지진에 적용 가능성을 평가하기 위해 역산 해의 안정성에 가장 큰 영향을 주는 요소인 속도 구조 모델에 대한 민감도를 분석하였다. 민감도 분석 결과를 통해 속도 구조 모델이 실제 속도 구조와 크게 어긋나지 않을 경우 실제 지진에 대해서도 충분히 적용 가능하다는 것을 확인하였다. 향후 속도 구조가 비교적 잘 밝혀진 지역에 본 역산 방법을 적용 할 경우 중간 규모 지진의 단층 파쇄 효과를 효과적으로 추정할 수 있을 것으로 예상되며, 이를 통해 적용된 지역의 지진 발생 특성을 이해하는데 큰 도움을 줄 수 있을 것이다.

주요어: 단층 파쇄 방향성, 모멘트 텐서 역산, 지진원 시간 함수, full Newton method

中規模地震の破壊方向を決定する新しい波形インバージョン法：震源モデルに対する数値実験

兪承勳[1]・李濬基[1]

1 ソウル大学 地球環境科学科

要 旨: 地震時における震源断層破壊の方向性は、地震損害を推定するための重要なパラメータである。しかし、通常のモーメントテンソル法逆解析では、本当の断層面や震源破壊の方向性を決定することができない。これらの限界を克服するために、本研究では周波数領域における波形逆解析法を用いて中規模地震のモーメントテンソルと震源域での破壊方向を同時に決定するために、新しい逆解析アルゴリズムを開発した。様々な破壊速度を用いた単方向および双方向破壊モデルの数値実験により、本手法で断層面や震源破壊方向に関する曖昧さを解決できることが確認された。技術の適用可能性を確かめるために、解の安定性に最大の影響を与える速度構造モデルに対する感度をテストした。感度テストの結果、たとえ速度モデルが完璧でなくとも、本手法は適用可能であることが示された。この方法を速度モデルが精度良く決定されている地域に適用すれば、中規模地震の震源域での破壊方向を推定することができ、その地域の地震発生メカニズムの理解に大きく貢献するであろう。

キーワード: 震源断層破壊方向，モーメントテンソル法逆解析，フルニュートン法